Advances in Research

10(5): 1-8, 2017; Article no.AIR.34338
ISSN: 2348-0394, NLM ID: 101666096

Facile Preparation of a Nanostructured Silver Oxide from a Mixed Ligand Coordination Polymer: Characterization and Biological Activity

Maged S. Al-Fakeh[1,2*]

[1]Department of Chemistry, Faculty of Science, Qassim University, Saudi Arabia.
[2]Taiz University, Taiz, Yemen.

Author's contribution

The sole author designed, analyzed and interpreted and prepared the manuscript.

Article Information

DOI: 10.9734/AIR/2017/34338
Editor(s):
(1) Soumendra Karmahapatra, Department of Pharmacology, Ohio State university, Columbus OH, USA.
Reviewers:
(1) Nguyen Van Toan, Vietnam National University, Vietnam.
(2) F. Javier Lopez Jaramillo, Universidad de Granada, Spain.
(3) Alejandro Torres Castro, Universidad Autónoma de Nuevo León, Mexico.
(4) Ondrej Kvitek, University of Chemistry and Technology, Czech republic.
(5) Mazen Alshaaer, University of Aveiro, Portugal and Prince Sattam Bin Abdulaziz University, Saudi Arabia.
Complete Peer review History: http://www.sciencedomain.org/review-history/20087

Original Research Article

Received 24th May 2017
Accepted 7th July 2017
Published 17th July 2017

ABSTRACT

In this research, the synthesis of a silver coordination polymer derived from1,2-bis (4-pyridyl)-ethane (BPA) and benzimidazole (BIMZ) is reported. It was synthesized, characterized and used as a precursor for silver oxide nanoparticles by calcination. The as-obtained complex products was characterized by elemental analysis, FT-IR, UV-visible spectra fluorescence technique, thermal analysis and scanning electron microscopy (SEM). X-ray powder diffraction analysis (XRD) showed that the size of the silver oxide nanoparticles obtained is 29 nm. The oxide exhibits strong antimicrobial actions on some Gram-negative and Gram-positive bacteria.

Keywords: Coordination polymer; AgO-NPs; XRD; thermal studies; biological activity.

**Corresponding author: E-mail: alfakehmaged@yahoo.com;*

1. INTRODUCTION

Nanoparticle synthesis and properties of fundamental importance in the advancement of recent research, silver oxide nanoparticles having vast applications in the field of oxidation catalysis, sensors, fuel cells, photovoltaic cells, optical data storage system and antimicrobials [1-7]. Silver nanoparticles can effectively inhibit the growth of *Staphylococcus aureus* and *Escherichia coli* [8-11]. Silver oxide coating was reported to be effective in killing *S. aureus* and *E. coli* [12]. The antibacterial activity of the high valence silver oxides have been also studied and showed that they have strong bacterial effect [13-17]. Recently, Chemical properties and potential applications in the fields of electronics, catalysis and pharmaceuticals of nanoparticles have been studied intensively [18-20]. Metal coordination polymers have received considerable attention in coordination chemistry, because of their well-documented conducting, magnetic, nonlinear optical, porous, thermal, and fluorescence properties besides their biological activities [21]. The use of the bridging flexible ligand 1,2-bis (4-pyridyl)ethane leads to interesting polymeric networks with intriguing structures and potential applications especially in catalysis [22]. Benzimidazole nucleus imparts certain pharmaceutical and corrosion inhibition properties for compounds comprising this nucleus [23-25].In this paper, synthesis and characterization of a new coordination polymer derived from 1,2-bis(4-pyridyl)-ethane (BPA), benzimidazole (BIMZ) and Ag(I) are described. The resulting coordination polymer was used as a precursor for synthesis of the nanosized silver oxide.

2. EXPERIMENTAL SECTION

2.1 Chemicals

1,2-Bis(4-pyridyl)ethane was supplied from Sigma Aldrich. Benzimidazole was a E. Merck grade. $AgNO_3$ (99.9%) was purchased from Shanghai Reagent Co. The reagents and solvents employed were commercially available and used as received without further purification. Fig. 1 shows the structure of the ligands.

The C.H.N (carbon, hydrogen and nitrogen) were performed using Analyischer Funktions test Vario El Fab-Nr.11982027 elemental analyzer. Infrared spectrum was recorded as KBr disks (400-4000 cm^{-1}) with a FT-IR spectrophotometer model Thermo-Nicolet-6700 FTIR and the electronic spectrum was obtained using a Shimadzu UV-2101 PC spectrophotometer. Thermal studies were carried out in dynamic air on a Shimadzu DTG 60-H thermal analyzer at a heating rate 10℃ min^{-1}. XRD pattern was obtained by a diffractometer model PW 1710 control unit Philips, anode material Cu 40 K.V 30 M.A optics: automatic divergence slit. Scanning electron microscope was of the type JEOL JFC-1100 E ION SPUTTERING DEVICE, JEOL JSM-5400 LV SEM. SEM specimen was coated with gold to increase the conductivity.

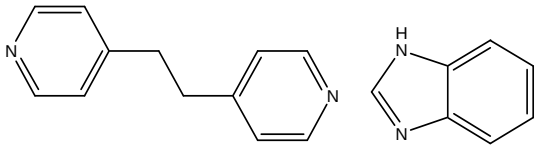

1,2-bis(4-pyridyl)-ethane
BPA

Benzimidazole
BIMZ

Fig. 1. Chemical structure of ligands

2.2 Antibacterial Activity

The disc-diffusion method was used to measure the antibacterial activity. The antibacterial activity of the silver oxide NPs was tested with some strains of bacteria namely: *Bacillus cereus* (G+ve), *Staphylococcus aureus* (G+ve), *Escherichia coli* (G-ve), *Pseudomonas aeruginosa* (G-ve) and *Serratia marcescens* (G+ve). Chloramphenicol was used as an antibacterial standard. The nutrient agar medium and nutrient broth medium were autoclaved for 20 min at 121℃ and 15 1b pressure before inoccupation then preparing a suspension of the bacterial strains in nutrient broth medium after cooling in a test tube. 0.3 ml from the suspension of bacterial strain were taken in petri dishes then the nutrient agar was poured onto the plate and the petri dish was shacked well and allow it to solidify. The plates were then kept in an incubator at 37℃. The width of the growth of inhibition zone around the disc was measured after 24 h incubation. To prepare inocula for bioassay, bacterial strains were individually cultured for 48 h in 100 ml conical flasks containing 30 ml nutrient broth medium [26].

2.3 Synthesis of [Ag (BPE)(BIMZ)(NO_3)]

BPA (2 g, 10.8 mmol) dissolved in 30 ml ethanolic solution was added to 20 ml of $AgNO_3$ (1.84 g, 10.8 mmol). The solution mixture was then stirred for about 15 min and an ethanolic

solution of BIMZ (1.28 g, 10.8 mmol) was then added. The solution mixture was heated on a water bath for about 50 min whereupon a white precipitate was separated which was filtered off, washed with ethanol and dried over $CaCl_2$. Anal. Calc. for $C_{19}H_{18}N_5O_3Ag$: C, 48.32; H, 3.84; N, 14.83. Found: C, 47.89; H, 3.62; N, 14.67. IR data: v(cm^{-1}) = 3510(w), 3432(w), 3068(m), 1614(s), 1558(s), 1420(m), 1390(s), 1220(s), 1168(m), 1070(m), 1010(s), 980(s), 812(s), 718(s), 676(s), 534(m), 510(w), 422(m).

2.4 Formation of Silver Oxide Nanoparticles

Calcination of the prepared coordination polymer in air at 500℃ with a calcination time of 3 hours afforded AgO nanoparticles.

3. RESULTS AND DISCUSSION

The reaction between silver nitrate and 1,2-bis (4-pyridyl)-ethane and benzimidazole proceeds readily to form the mixed ligand complex. This compound is stable in air and partially soluble in DMSO.

3.1 Fourier Transform Infrared Spectroscopy (FT-IR)

The main IR bands of the prepared compound are cited in the experimental part. The band observed at 1614 cm^{-1} region is assigned to the u(C=N) stretching vibration of the BPA [27]. BIMZ exhibits two bands at 980 and 1420 cm^{-1} which can be attributed to u(C-N) ring vibrations [28] (Fig. 2). The metal-nitrogen stretching frequency is located at 412 cm^{-1}, associated with the vibration of the M-N bond [29].

3.2 Electronic Spectra

The electronic spectrum of the mixed ligand compound is recorded in dimethyl sulphoxide (DMSO). The spectrum of the complex displays two distinct bands at 34,482 and 25,235 cm^{-1} which are attributed to π→π* and n→π* transitions within the BPA and BIMZ moieties, respectively [27,28]. The structure of the silver coordination polymer can be postulated in Fig. 3.

3.3 Thermal Analysis

In dynamic air the thermal decomposition of the silver (I) compound has been investigated from ambient temperature to 650℃. The thermogram of this complex shows two decomposition steps (Fig. 4) at 32-298 and 299-650℃. The first stage corresponds to decomposition of the BIMZ ligand (calc. 25.01%, found 24.75%). The DTG curve displays this step at 240℃and correspondingly an exothermic peak at 242℃ was recorded in the DTA trace. The second step represents a mass loss indicating the decomposition of the ligands (calc. 52.14%, found 50.49%) (DTG peaks at 430℃) with an exothermic peak in the DTA trace at 432℃. The final product was identified on the basis of mass loss consideration as silver oxide (calc. 26.22%, found 25.75%). The non-isothermal kinetic analysis of the silver complex was carried out applying the Coats-Redfern [30] method. The kinetic parameters of the silver (I) compound is calculated for the first step and are cited in Table 1.

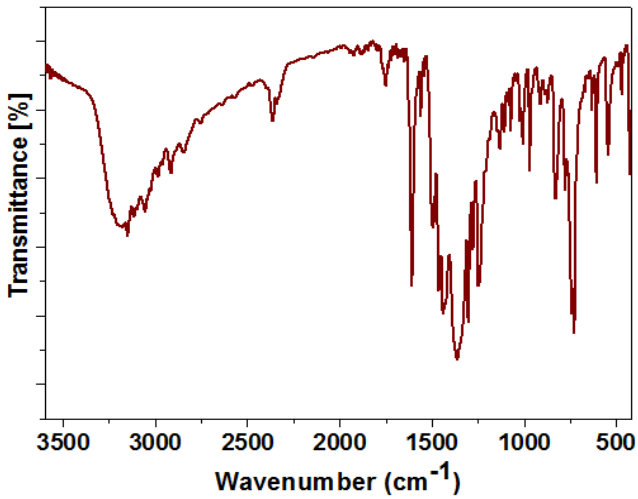

Fig. 2. FT-IR of Ag(I) complex

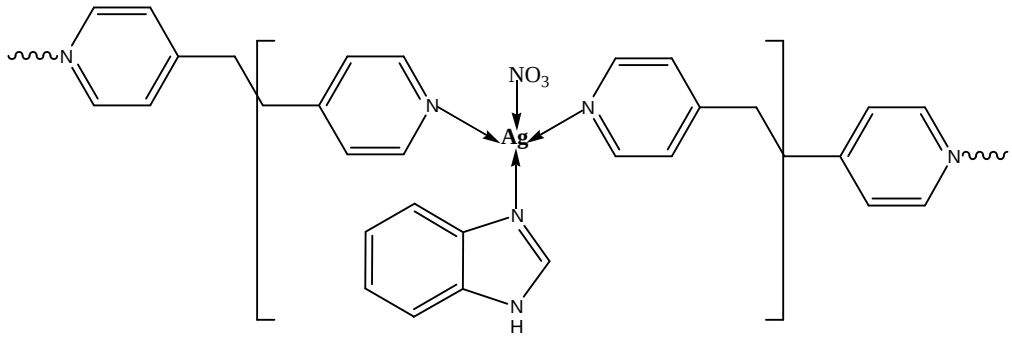

Fig. 3. Structure of $[Ag(BPA)(BIMZ)(NO_3)]_n$

Table 1. Kinetic and thermodynamic parameters for the thermal decomposition of the Ag (I) compound

Step	Coats-Redfern equation				ΔS*	ΔH*	ΔG*
	r	n	E	Z x 10^2			
	0.9968	0.00	61.81	12.41	-205.82	57.59	161.94
	0.9975	0.33	66.56	13.31	-184.29	62.34	155.77
1st	0.9976	0.50	69.42	13.88	-183.94	64.20	157.45
	0.9978	0.66	71.64	14.31	-183.69	67.42	160.55
	0.9982	1.00	77.03	15.38	-183.09	72.81	165.63
	0.9991	2.00	94.46	18.77	-181.43	90.24	182.22

E in kJ mol^{-1}, underlined r in all tables represents the best fit values of n and E
ΔH, ΔG* are in kJ mol^{-1} and ΔS* in kJ mol^{-1} K^{-1}*

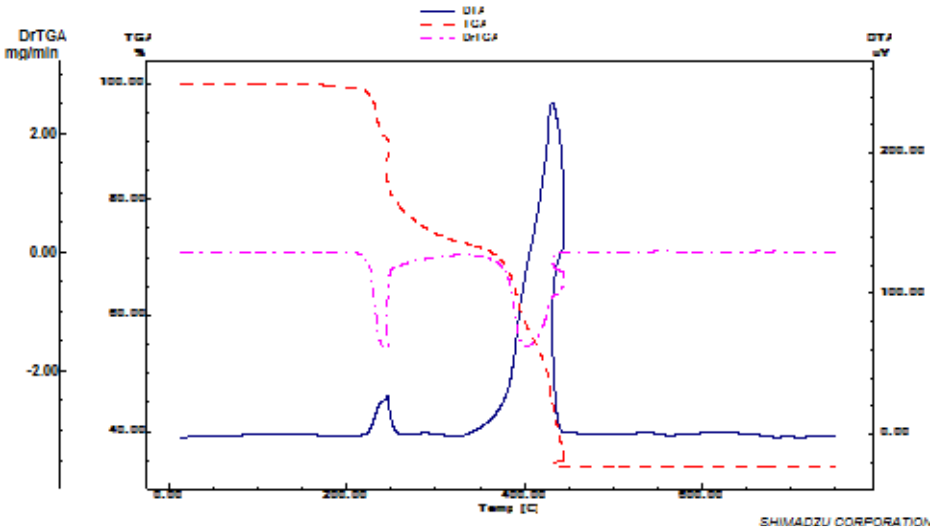

Fig. 4. TG, DTG and DTA thermograms of the Ag(I) compound in dynamic air

3.4 X-ray Powder Diffraction of Silver Oxide

The X-ray powder diffraction pattern was recorded for the AgO nanoparticles. The crystal data for AgO NPs belong to the monoclinic system. The significant broadening of the diffraction patterns suggests that the particles are of the nanometer dimensions. XRD pattern is depicted in Fig. 5. The following Scherrer's equation was applied to estimate the particle size of the compound:

$$D = K\lambda / \beta\cos\theta$$

where K is the shape factor, λ is the X-ray wavelength typically 1.54 Å, β is the line broadening at half the maximum intensity in radians and θ is Bragg angle, D is the mean size of the ordered (crystalline) domains, which may be smaller or equal to the grain size. The crystal data together with the particle size (29 nm) are recorded in Table 2.

3.5 Scanning Electron Microscopy (SEM)

The scanning electron microscopy of silver oxide nanoparticles is given in Fig. 6. In order to elucidate the AgO nanoparticle morphologies, scanning electron microscopy (SEM) was performed which demonstrates clearly the formation of AgO nanostructures for the sample calcined at 500℃ for 3 h.

Table 2. X-ray diffraction crystal data of the AgO NPs

Parameters	AgO
Empirical formula	AgO
Crystal system	monoclinic
a (Å)	5.859
b (Å)	3.484
c (Å)	5.449
α (°)	90.00
β(°)	107.51
γ(°)	90.00
Particle size(nm)	29

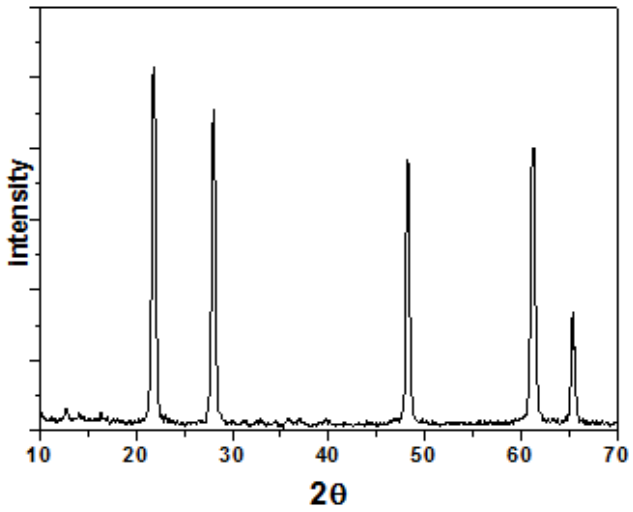

Fig. 5. XRD of AgO nanoparticles

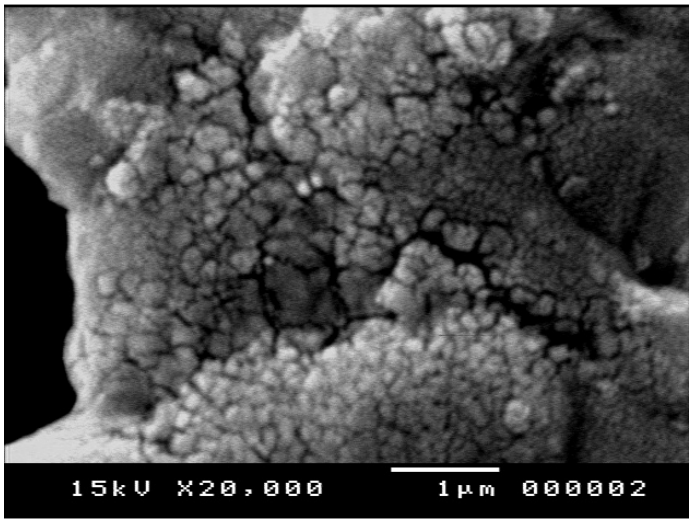

Fig. 6. SEM of silver oxide nanostructures

The SEM micrograph indicates that there are many micropores among the nanocrystals for the oxide.

3.6 Antimicrobial Activity

The antimicrobial activity of the silver oxide nanostructures was investigated against five bacterial strains Table 3. In the literature there are a number of studies in the field of silver oxide nanoparticles by using different types of procedures [31-35]. In testing the antibacterial activity of the AgO NPs in this work, more than one test organism were used to increase the chance of detecting the antibiotic principles in the tested materials. The data showed that in some cases the silver oxide nanostructures possess a similar and higher antimicrobial activity than the selected standard (chloramphenicol) especially against *Serratia marcescens* (-ve) and *Pseudomonas aeruginosa* (-ve). Figs. 7 & 8 show the antibacterial effect for AgO nanostructures.

Table 3. Microbiological screening of the AgO nanostructures

Compound	*B. Cereus* (G+ve)	*S. aureus* (G+ve)	*S. Marcescens* (G-ve)	*E. coli* (G-ve)	*P. aeruginosa* (G-ve)
AgO	22	17	**30**	14	**22**
Cont.*	30	24	34	25	15

Cont. = Chloramphenicol as antibacterial standard

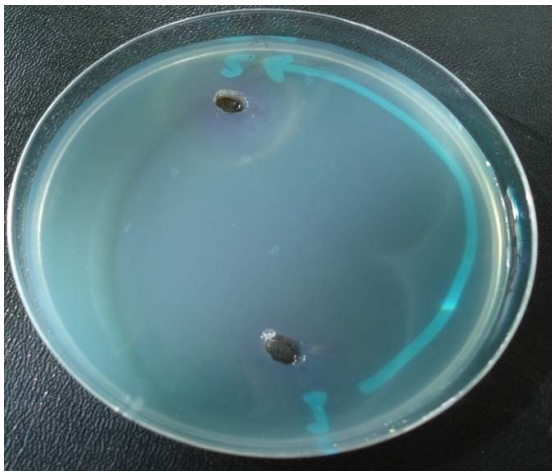

Fig. 7. Microbiological screening of the silver oxide nanostructures against *Pseudomonas aeruginosa* (-ve)

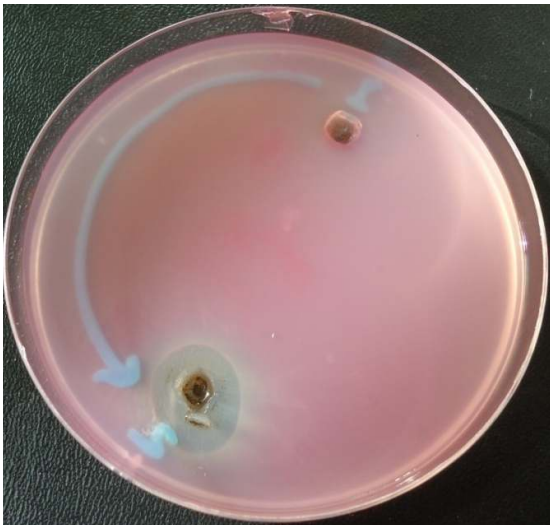

Fig. 8. Microbiological screening of the silver oxide nanostructures Against *Serratia marcescens* (-ve)

4. CONCLUSION

In conclusion a Ag(I) coordination polymer derived from 1,2-bis(4-pyridyl)-ethane and benzimidazole ligands could be synthesized and structurally characterized. We have successfully prepared the silver oxide nanostructures by calcinations of this coordination polymer. X-ray powder diffraction analysis reveals that the crystallite size of the AgO particles was found to be 29 nm.

COMPETING INTERESTS

Author has declared that no competing interests exist.

REFERENCES

1. Derikv F, Bigi R, Maggi, Piscopo CG, Sartori G. Oxidation of hydroquinones to benzoquinones with hydrogen peroxide using catalytic amount of silver oxide under batch and continuous-flow conditions. Journal of Catalysis. 2010; 271:99-103.
2. Wang W, Zhao Q, Dong J, Li J. A novel silver oxides oxygen evolving catalyst for water splitting. International Journal of Hydrogen Energy. 2011;36:7374-7380.
3. Petrov VV, Nazarova TN, Korolev AN, Kopilova NF. Thin sol–gel SiO_2–SnOx–AgOy films for low temperature ammonia gas sensor, Sensors and Actuators B:

Chemical. Sensors and Actuators B. 2008;133:291–295.
4. Sanli E, Uysal BZ, Aksu ML. The oxidation of $NaBH_4$ on electrochemicaly treated silver electrodes. International Journal of Hydrogen Energy. 2008;33:2097.
5. Ida Y, Watase S, Shinagawa T, Watanabe M, Chigane M, Inaba M, Tasaka A, Izaki M. Chemistry of Materials. 2008; 20:1254.
6. Joachim Schnadt, Jan Knudsen, Xiao Liang Hu. Experimental and theoretical study of oxygen adsorption structures on Ag(111). Physical Review B. 2009;80: 075424 .
7. Gu YHWHY. Microchimica Acta. 2009;164:41.
8. Panacek A, Kolar M, Vecerova R, Prucek R, Soukupova J, Krystof V, Hamal P, Zboril R, Kvitek L. Antifungal activity of silver nanoparticles against *Candida* spp. Biomaterials. 2009;30:6333.
9. Cho KH, Park JE, Osaka T, Park SG. The study of antimicrobial activity and preservative effects of nano silver ingredient. Electrochim. Acta. 2005;51:956.
10. Mirzajani F, Ghassempour A, Aliahmadi A, Esmaeili MA. Antibacterial effect of silver nanoparticles on *Staphylococcus aureus.* Res. Microbiol. 2011;162:542.
11. Chamakura K, Perez-Ballestero R, Luo ZP, Bashir S, Liu JB. Comparison of bactericidal activities of silver nanoparticles with common chemical disinfectants. Colloid Surf. B Biointerfaces. 2011;84:88.
12. Li YN, Sun YZ, Zhang YS, Du LP, Sun Y, He QH. Chin. J. Vac. Sci. Technol. 2011;31:129.
13. Soheyla khezli, Ali Abedini. Effect of amino acids as a capping agent on the size and morphology of pure AgO nanoparticles and its photocatalyst application. J Mater Sci: Mater Electron. 2017;28:10535.
14. Lalueza P, Monzon M, Arruebo M, Santamaria J. Bactericidal effects of different silver-containing materials. Mater. Res. Bull. 2011;46:2070- 2076.
15. Shen WN, Feng LJ, Kong ZZ, Feng H. Acta Chim. Sin. 2011;69:277.
16. Li Q, Chen K, Jiao LL, Zhou GG. Technology. 2008;27:12.
17. Sobhani-Nasab Ali, Mohsen Behpour. Synthesis, characterization and morphological control of nanoparticles through green method and its photocatalyst application. J Mater Sci: Mater Electron. 2016;27:1191.
18. Kazemi H, Zandi K, Momenian H, J. Nanostruct. 2015;5:25.
19. Nikkaran AR, Mir N, Nejati-Yazdinejad M, Mir AA, J. Nanostruct. 2013;3:341.
20. Rosi NL, Mirkin CA. Nanostructures in biodiagnostics. Chem. Rev. 2005;105: 1547.
21. Janiak C, Dalton Trans. Engineering coordination polymers towards applications. Dalton Transactions 2003; 2781.
22. Soo Hyun Kim, Byeong Kwon Park, Young Joo Song. Construction of crystal structures of metal (II)–benzoates (M = Mn, Ni, Co, Cu, Zn, and Cd) and 1,2-bis(4-pyridyl)ethane: Effects of metal coordination modes and their catalytic activities. Inorganica Chimica Acta. 2009;362:4119.
23. Rajendiran V, Murali M, Suresh E. Mixed ligand ruthenium (II) complexes of bis(pyrid-2-yl)-/bis(benzimidazol-2-yl)-dithioether and diimines: Study of non-covalent DNA binding and cytotoxicity. Dalton Trans. 2008;7:148.
24. Mann J, Baron A, Opoku-Boahen Y, Johansson E, Parkinson G, Kelland LR, Neidle S. A new class of symmetric bisbenzimidazole-based DNA minor groove-binding agents showing antitumor activity. J. Med. Chem. 2001;44:138.
25. Goudgaon NM, Dhondiba V, Vijayalaxmi A. Indian J. Heterocycl. Chem. 2004;13:271.
26. Kwion- Chung, Bennett; 1992.
27. Alireza A, Ali M, Veysel TY, Orhan B, Inorganica Chimica Acta. 2009;362:1506.
28. Banu KS, Mondal S, Guha A, Das S. Polyhedron. 2011;30:163.
29. Ng Law Yong, Akil Ahmad, Abdul Wahab Mohammad. Synthesis and characterization of silver oxide nanoparticles by a novel methods. International Journal of Scientific & Engineering Research. 2013;4(5).
30. A. Coats and J. Redfern, Nature. 1964;20: 68.
31. Krishnamoorthy P, Jayalakshmi T. Journal of Chemical and Pharmaceutical Research. 2012;4(11):4783.
32. Jain D, Kachhwaha S, Jain R, Srivastava G, Kothari SL. Novel microbial route to synthesize silver nanoparticles using spore crystal mixture of Bacillus thuringiensis. Indian Journal of Experimental Biology. 2010;48:1152.
33. Das R, Nath SS, Chakdar D, Gope G, Bhattacharjee R. Preparation of silver

nanoparticles and their characterization. Journal of Nanobiotechnology. 2009;5.
34. Kiruba Daniel SCG, Anitha Sironmani T. Synthesis and characterization of fluorophore attached silver nanoparticles. Bull. Mater. Sci. 2011; 34(4):639.
35. Singh A, Jain D, Upadhyay MK, Khandelwal N, Verma HN. Green synthesis of silver nanoparticles using Argemone Mexicana leaf extract and evaluation of their antimicrobial activities. Digest Journal of Nanomaterials and Biostructures. 2010;5(2):483.

Peer-review history:
The peer review history for this paper can be accessed here:
http://sciencedomain.org/review-history/20087